

# MODELLING OF COMPACT RANGE QUIET-ZONE FIELDS BY PO AND GTD

Frank Jensen\*, Laurent Giauffret\*\* and Javier Martí-Canales\*\*\*

\*TICRA, Kronprinsensgade 13, DK-1114 Copenhagen K, DENMARK, e-mail: ticra@ticra.com

\*\*Satimo, Place du Ségala, F-46500 Gramat, FRANCE, e-mail: satimo.lot@wanadoo.fr

\*\*\*ESTEC, NL-2200 AG Noordwijk ZH, THE NETHERLANDS, e-mail: jmartica@estec.esa.nl

## Abstract

**Modelling of the field in the quiet zone (QZ) of a compact range is a difficult task since the edges of the range reflectors are designed not to radiate into the quiet zone. As a consequence the edges of the range reflectors are complicated to model electromagnetically.**

**In the present paper we compare modelling by physical optics (PO) with modelling by the uniform geometrical theory of diffraction (GTD). The investigation is carried out on a double reflector range with rectangular serrated reflectors. It is found that the range far field determined by PO is best explained by a ray model for reflectors having a double straight edge, which suggests to apply a GTD model on reflectors with straight edges but with attenuated diffraction contribution.**

**Both PO and GTD results are shown and compared to measurements.**

*Keywords: Compact range evaluation, Compact range modelling, Serrated edge modelling.*

## 1. Introduction

In an ongoing study for ESA (ESTEC Contract No. 12878/NL/NB) Satimo and TICRA investigate the possibilities for correcting compact range measurements for polarization errors. This involves a careful modelling of the QZ field in the compact range in order to describe the in-

completeness of the field. In the following the results of such modelling will be discussed.

The QZ field of a compact range shall represent a plane wave and this is generated by one or more reflectors. An ideal plane wave is, however, unlimited in width, so the problem of the range design is to construct limits for the plane wave without degrading it.

Two basic designs exist here. In the rolled-edge design the ideal reflector surface is gradually bent to the rear. Hereby the field is reflected away from the QZ until it disappears in the backward direction. No rays from the rolled edge area will reflect into the QZ.

The alternative is the serrated edge where the edge is cut in teeth with edges mainly perpendicular to the straight edge. Hereby all the diffractions are scattered away from the QZ.

Thus, in an electromagnetic modelling of the range, ray methods such as GTD will not give a contribution to the QZ field from the edges. Then a surface integration technique as PO may be applied but a detailed modelling of especially the edge serrations includes so many and fine details that it is difficult to trust the method.

The edge treatment therefore calls for simplified solutions both by PO and by GTD. In the present paper PO and GTD methods based on the smooth reflector edge will be presented and compared to measurements.

## 2. Determination of the QZ field

The quiet-zone field of a compact range may be modelled essentially by three different methods.

The first method is based on geometrical optics (GO), which is employed in the basic design of the compact range. When GO is applied in modelling of the quiet-zone field it

will only show the smooth field variation caused by the taper of the feed. The typical field ripples characterising a true QZ field cannot be modelled by GO. These ripples are mainly generated by the edges of the main reflector.

GO may be combined with GTD whereby edge effects are included; but in general the edges of the range reflectors are difficult to model by GTD. For reflectors with rolled edges these are constructed with such a smooth transition between the central reflector and the rolled edge section that diffractions will not occur, at least not from known diffraction coefficients. For reflectors with serrated edges the serrations have corners and tips, which are small compared to the wavelength and they can therefore not be represented accurately by GTD.

The last method is physical optics (PO) in which the currents on a reflector are determined and integrated to give the field either on the subsequent next reflector or in the quiet zone. In general the method is very accurate although it assumes that the surface currents near the edge of a reflector are not affected by the edge, which is obviously incorrect. Further, PO may be very time consuming for large reflectors, as the integration grid needs to be fine when the near field shall be determined.

Modelling of rolled edges by PO is possible when the surface is known but it is difficult to specify the point at which the surface rolls back into the shadow from the illuminating source.

For serrated reflectors it is more complicated and it is a difficult task to model each tooth of the serrations (cf. Chang and Im [1]). The scattering from the serrated area will consist of a surface-reflected contribution and a contribution from diffractions in the edges of the teeth. With a proper design the latter will not radiate into the QZ and is then less important. At some distance from the teeth the former will be smeared out. It may, therefore, be modelled by applying the surface currents for a solid reflector weighted by the relative solid area of the serrations. For teeth with straight edges the weight will be linear, decreasing from unity at the root of the teeth to zero at the tips. This modelling is adopted in the following PO calculations.

All calculations presented were carried out by GRASP8 [2].

### 3. Sample case: The CATR at ESTEC

As computational example, the Compact Antenna Test Range (CATR) at ESTEC has been chosen. This range consists of two singly curved parabolic reflectors with serrated

edges [3,4]. The subreflector collimates the feed radiation to a horizontal field and the main reflector collimates the field to a limited width, cf. Figure 1.

The main reflector has a height of 2500 mm and a width of 4000 mm. These measures are reduced by the serrations, which are 400 mm on the main reflector. The subreflector is slightly oversized, i.e. the GO rays to the main reflector edge reflect inside the edge of the subreflector. The resulting aperture size of the solid part of the main reflector is then 1700 mm by 2688 mm. Including the serrations the aperture is 2500 mm by 3360 mm as illustrated in Figure 1.

The range feed is linearly polarized and has a taper of -2 dB in the E-plane. In the modelling the H-plane taper is -2.2 dB causing realistic cross-polarization lobes of -35 dB in the 45° planes. Further, an on-axis cross-polarization at -40 dB is modelled, see Figure 2.

Scattering in e.g. the walls and the AUT positioner is not included in the presented modelling.

## 4. Measurements

The chamber has recently been refurbished and measurement results in linear polarizations are available at 9.35 GHz for a horizontal and a vertical scan in the quiet zone 4560 mm in front of the centre of the main reflector [5]. The calculated QZ fields will be compared to these measurements.

## 5. PO-PO modelling

The QZ field of the CATR has been determined fully by PO. Thus, first the currents on the subreflector are calculated from the feed illumination, next these currents illuminate the main reflector and the resulting currents on the main reflector are calculated. Finally, from the latter currents the QZ field is determined. The effect of the serrations is included by weighting the currents linearly over the serrated area of both reflectors.

The calculated QZ field in a horizontal plane is shown in Figures 3 and 4 for horizontal and vertical range polarizations, respectively, together with the measured results. A qualitatively good agreement is found. Differences between the two polarizations are due to different feed taper, polarization dependent contributions from the edges, and spurious signals. It is striking that the calculated results are very alike for the two polarizations, which shows that the edge effects have been effectively removed in the modelling.

The agreement between the model and the measurements is less convincing in the vertical cut, Figure 5, in which the PO-PO model shows very strong ripples while the measurements show small variations.

## 6. GO-PO modelling

A simpler calculation is obtained by modelling the subreflector by GO. Thus the currents on the main reflector are determined directly from the feed radiation reflected in the subreflector. The serrated area of the subreflector is then considered as solid and edge effects from the subreflector are neglected. The QZ field is determined by applying PO on the main reflector as before. The results are shown in Figure 6 and the simpler GO-PO method shows a better agreement with the measurements for horizontal range polarization than the PO-PO model. However, this is not found for the vertical range polarization.

In the vertical cut, Figure 5, the GO-PO model shows a better agreement to the measurements than the PO-PO model did.

The fact that the GO-PO model is better than the PO-PO model suggests a ray interpretation of the field propagation through the range. In the horizontal plane a GO analysis shows, cf. Figure 1, that the rays to the edge area of the main reflector are reflected within the solid area of the subreflector. The GO analysis of the subreflector is thus realistic.

In the vertical plane we find that the rays, which are GO reflected in the serrated area of the subreflector also hit the serrated area of the main reflector. As the PO modelling weights the currents over the serrated area it is the same rays which are weighted both on the subreflector and on the main reflector. This squared weight will be steep at the base of the serrations and this may in the modelling result in a partial elimination of the serrations resulting in the strong ripples in the vertical patterns.

## 7. Far field by PO-PO

For further evaluation of the range the far field (at 12 GHz) has been calculated by PO on both the subreflector and on the main reflector. A horizontal cut in the far field is shown in Figure 7 where we find side lobes at oscillating levels. The lobe pattern can be explained from the serration model, which gives the aperture distribution a discontinuous derivative at the root of the serrations where the weighting starts. The aperture then has two characteristic widths,  $D_1$

including and  $D_2$  excluding the serrations. The two apertures cause far-field lobes given by

$$\sin(\pi u_i)/(\pi u_i) \quad \text{where } u_i = (D_i/\lambda)\phi, \quad i=1,2,$$

$\phi$  being the horizontal far-field angle. Neglecting the nominator, the sum of the two sine functions can be written as the product of  $\sin(\pi u_+)$  and  $\cos(\pi u_-)$  where

$$u_+ = (u_1+u_2)/2 \cong ((D_1+D_2)/2\lambda)\phi = (D/\lambda)\phi \quad \text{and} \\ u_- = (u_1-u_2)/2 \cong ((D_1-D_2)/2\lambda)\phi = (L/\lambda)\phi,$$

$D$  being the width between the centres of the serrations and  $L$  the width of the serrations in the aperture plane.

The narrow lobes in the pattern are then spaced by  $\lambda/D = 25\text{mm}/3024\text{mm} = 0.47^\circ$  and the wide lobes of the envelope are spaced by  $\lambda/L = 25\text{mm}/336\text{mm} = 4.3^\circ$  in agreement with the calculated far field, Figure 7.

In a vertical cut the lobes are quite different. This is most easily observed in a contour plot of the far field around the main lobe, Figure 8. The groups of narrow lobes in the horizontal plane are seen in agreement with Figure 7, but in the vertical direction the narrow lobes follow a curve to the right while some wider lobes follow a curve slightly bending to the left.

Though calculated by PO this is explained most easily by a ray interpretation. All rays from the subreflector are horizontal. The vertical edges of the main reflector will then diffract only in the horizontal plane as already observed. The horizontal edges of the main reflector will diffract in a cone, which in average has an opening angle of  $57^\circ$  and which cuts the far-field sphere in the right-bending curve of Figure 8. The lobe widths along the curve are  $0.85^\circ$  corresponding to an effective height of 1700 mm, which is the height of the main reflector without serrations. The results are calculated by PO-PO, which, cf. Section 6, to a high degree ignores the serrations.

The other row of lobes bending to the left follows precisely the trace of the diffraction cones from diffractions in the horizontal edges of the subreflector followed by reflection in the main reflector. The width of the lobes,  $4.7^\circ$ , corresponds to the height of the serrations on the subreflector, 300 mm.

Of the rays from the lower subreflector edge only those above horizontal level will be reflected in the main reflector and radiate in the upper part of the contour diagram. Correspondingly, the rays from the upper edge of the subreflector will radiate in the lower part of the contour diagram. Thus, the rays from the upper and lower subreflector edge do not interfere and narrow lobes do not occur.

## 8. GO-GTD modelling

As the PO-PO far field is successfully explained by GTD rays from rectangular reflectors it is reasonable to try to model the compact range by GTD on reflectors with straight edges along the centre lines of the serrations. However, The edge contributions shall be attenuated suitably. Here good results have been obtained by attenuating the diffracted signals by 20 dB.

Calculation of the QZ near field with GO on the subreflector and GTD on the main reflector results in the fields shown in Figure 9 for horizontal range polarization. The agreement with the measurements is reasonable and as good as for the previous models.

## 9. Longitudinal cut in the QZ

The variation of the QZ field down through the range is rather slow as shown in Figure 10, which shows a comparison between the results for the GO-PO model and the GO-GTD model. The periods in the ripples of the field are clearest in the GO-GTD model and are related to the main-reflector edge-diffracted rays of which precisely four exist. The closer the edge, the shorter the period. GO-PO gives a field with less distinct periods but qualitatively alike the GO-GTD field.

## 10. Conclusion

In the present paper the electromagnetic modelling of a compact range consisting of two serrated single-curved reflectors has been investigated. In the PO method the serrations of the reflectors have been modelled by giving the surface currents a relative weight proportional to the solid area of the serrations. Applying GO on the subreflector and this PO model on the main reflector gives slightly better results than applying PO on both reflectors.

It has been very rewarding to interpret the PO results from a ray-tracing point of view. Subsequent GTD computations on the main reflector modelled with straight edges along the centre line of the serrated areas and with the edge diffracted field attenuated by 20 dB turns out to give results which, when compared to measurements, are as good as the PO based results. The ripples in the calculated QZ field have correct amplitude but the lobe distance seems to be too short, which indicates that the modelled aperture of the range is larger than the effective aperture.

The ray interpretation suggests future investigations in

which the reflectors have a double rim, one at the base of the serrations and one at the tips. Such a modelling is planned in the near future.

## References

- [1] Yueh-Chi Chang and Myung Jin Im, "A PTD analysis of serrated edge compact range reflectors", in *Proc. of AMTA 16th Meeting and Symposium*, pp.175-179, Long Beach, October 1994.
- [2] Knud Pontoppidan (ed.), *Technical description of GRASP8*, Report S-894-02, TICRA, Copenhagen, July 1999.
- [3] S.C. van Someren Greve, V.J. Vokurka and J. Torres, *Mini compact antenna test range*, Final report on ESA Contract 6179/85/NL/GM, March Microwave Systems B.V., Nuinen, The Netherlands, June 1987.
- [4] V.J. Vokurka, "Compact-antenna range performance at 70 GHz", in *IEEE International Symposium on Antennas and Propagation*, Digest pp.260-263, Québec, June 1980.
- [5] Javier Martí Canales, *CATR Quiet Zone Characterization*, Test Report CATR/TR/003.97/JM, EMC and Antenna Measurement Section, ESTEC, The Netherlands, May 1997.

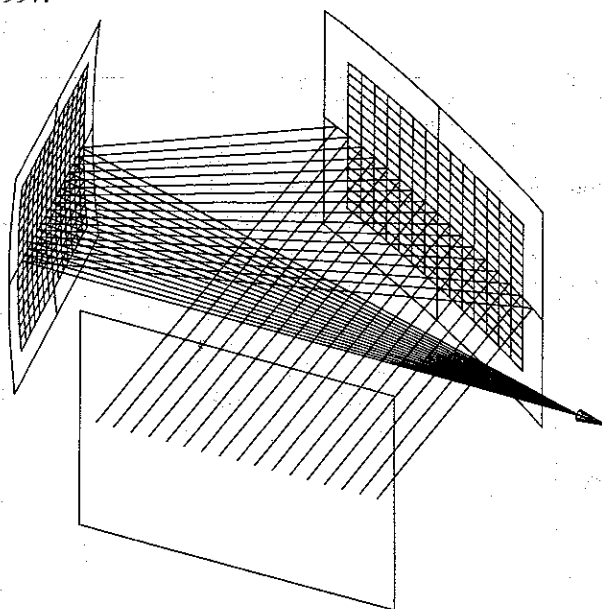


Figure 1 The model of the CATR at ESTEC. Rays from the feed to a horizontal cut in the QZ are shown, the width of the cut is  $\pm 1500$  mm. The rectangle in the QZ is the aperture of the main reflector including serrations. The white borders of the reflectors illustrate the serrated areas.

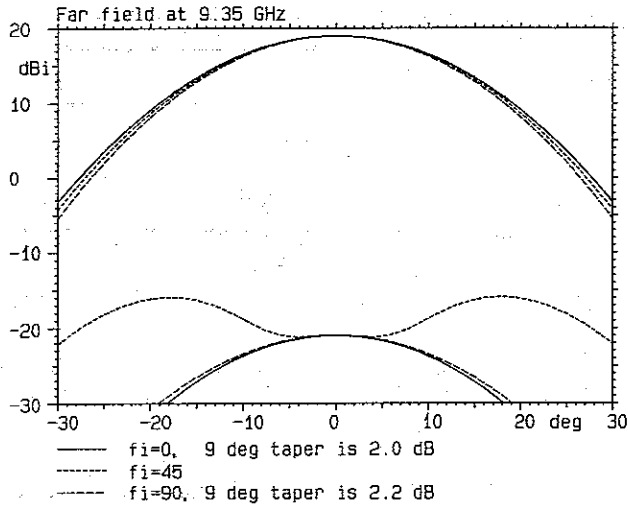


Figure 2. Co- and cross-polar pattern of the range feed.

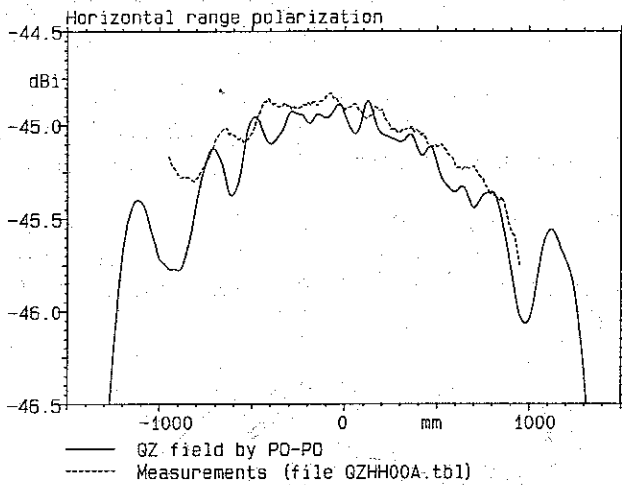


Figure 3. QZ field calculated by PO-PO compared to measurements; horizontal cut, horizontal range polarization.

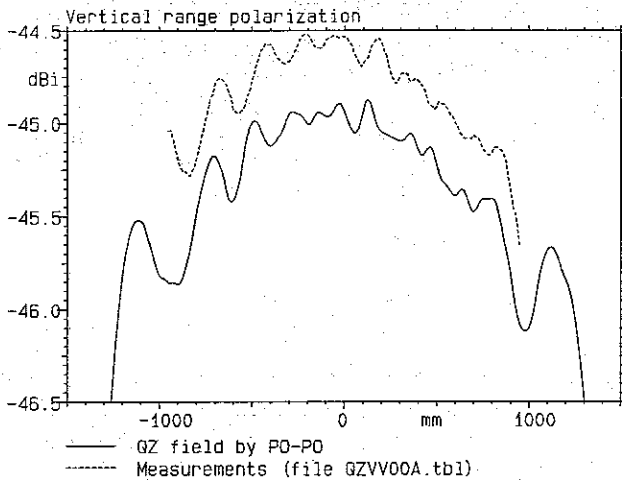


Figure 4. QZ field calculated by PO-PO compared to measurements, vertical range polarization.

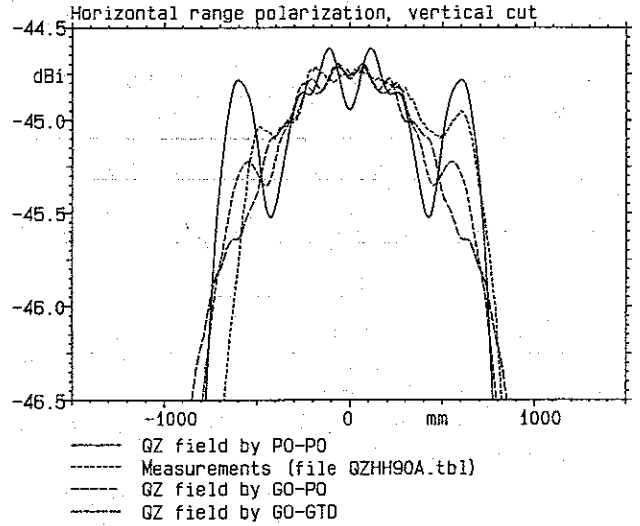


Figure 5. QZ field calculated by PO-PO, by GO-PO and by GO-GTD compared to measurements, vertical cut, horizontal range polarization.

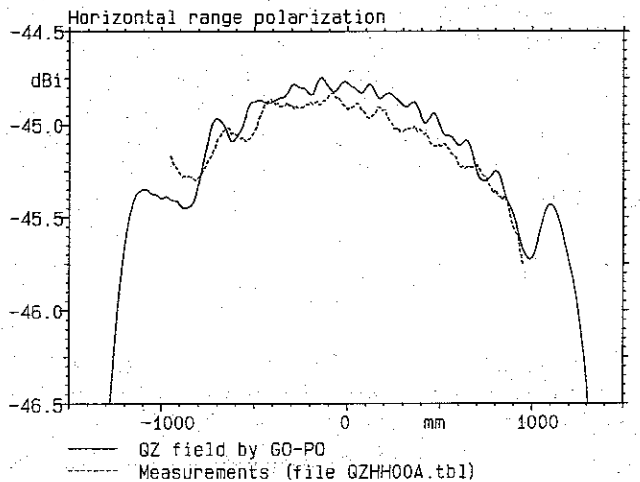


Figure 6. QZ field calculated by GO-PO compared to measurements, horizontal range polarization.

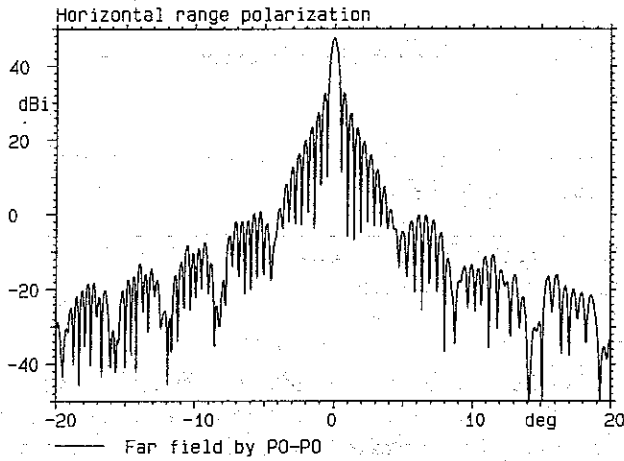


Figure 7 CATR far field calculated by PO-PO, horizontal cut, horizontal range polarization (12 GHz).

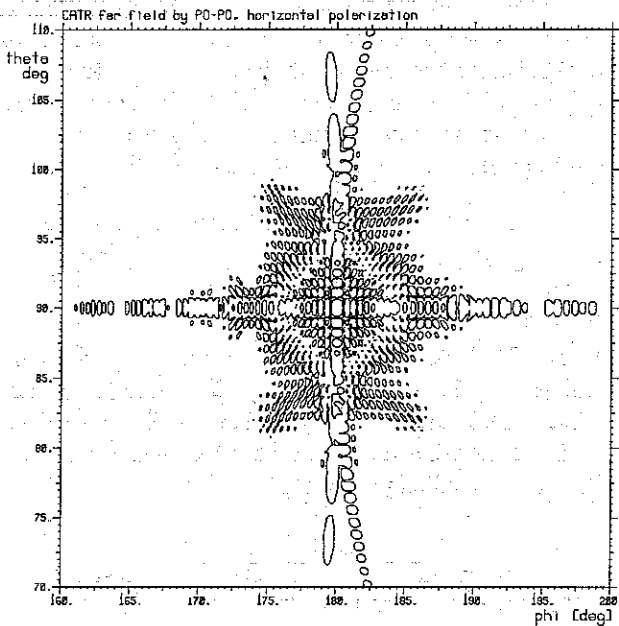


Figure 8 Contour plot of the PO-PO calculated co-polar field at horizontal range polarization.

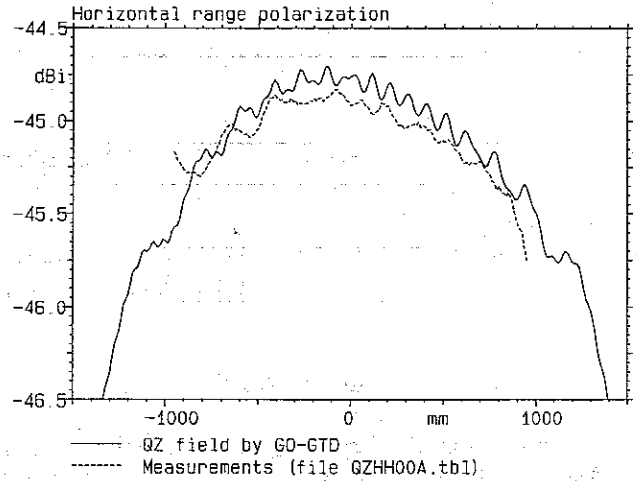


Figure 9 QZ field calculated by GO-GTD compared to measurements, horizontal range polarization.

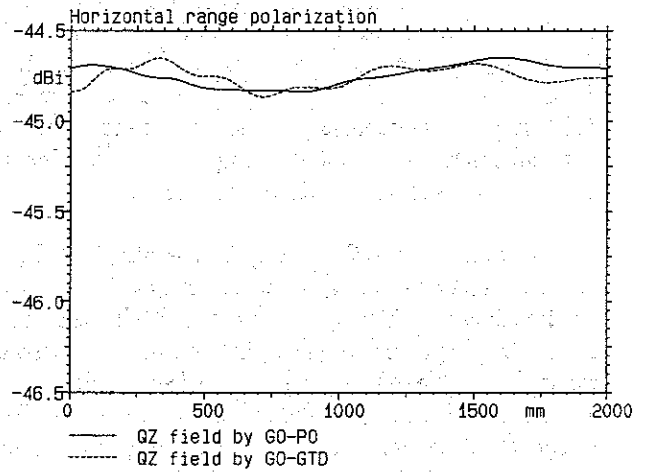


Figure 10 QZ field along a longitudinal QZ cut by GO-PO and by GO-GTD, horizontal range polarization. The cut is for  $x=-130$  (abscissa in Figure 3) and  $y=0$  (abscissa in Figure 5). These previous figures are for  $z=1150$ , the abscissa of this figure.